

DIURNAL AND LONG-TERM VARIATIONS OF THE KINETIC ENERGY GENERATION AND DISSIPATION FOR A FIVE-YEAR PERIOD

ERNEST C. KUNG*

Geophysical Fluid Dynamics Laboratory, ESSA, Washington, D.C.

ABSTRACT

The diurnal variation and long-term variation of the kinetic energy generation and dissipation are investigated with the wind and geopotential data observed twice a day at 00 and 12 GMT over North America during a 5-yr. period. The generation from the work done by the horizontal pressure force and the dissipation are significantly and consistently greater at 00 GMT than at 12 GMT. The diurnal variation is especially pronounced during the summer. The annual march of the seasons and the year-to-year variation of the kinetic energy parameters are also significant.

By the use of twice-a-day observations for an extended period, the study over North America is increased in generality as an approximation to hemispherical features. However, some uncertainty remains in this respect because of the possible effects of the semidiurnal variations and unconfirmed radiation errors in the radiosonde observations. The previously reported double maxima of the generation and dissipation in the planetary boundary layer and at the jet stream level derived from limited data are confirmed in this study. The multi-annual mean of the dissipation is estimated as 4.12 watts/m.² About half of the estimated dissipation takes place in the boundary layer, and the other half takes place in the free atmosphere.

1. INTRODUCTION

This paper reports further results of a continuing study of the problem of the large-scale energy generation and dissipation in the atmosphere. In one of the previous reports (Kung [10]), the kinetic energy generation, dissipation, and related energy parameters were studied in their various partitionings with 6 month's daily wind and geopotential data over North America. Of special interest in that paper was the devising of a technique to evaluate the cross-isobar flow, with which one may directly compute kinetic energy generation from observed wind and geopotential data at individual isobaric surfaces. This also suggested a feasible way of providing a broader observational basis for studying the problem of energy dissipation, since in this manner we can obtain the dissipation as the residual term to balance other energy parameters in the kinetic energy equation *without employing specific theories*.

In the following report (Kung [11]), the kinetic energy generation, local change, horizontal outflow, vertical transport, and dissipation were evaluated for 20 pressure layers from the surface to 50 mb. using 11 months' daily wind and geopotential data over North America. The vertical distribution and balance of the evaluated energy parameters and also the efficiency of the dissipation in different portions of the atmosphere were studied.

The data coverage in the previous studies was limited to North America for a relatively short period up to 11 months. The aerological data employed in the computational analysis were the rawinsonde/radiosonde observations taken once a day at 00 GMT. With the results of the study reported in the previous papers, it became highly desirable to do the energy budget study for a more extensive period, preferably with more than one observation per day. Since the dissipation is to be evaluated as the residual term in the kinetic energy equation at this stage, the evaluation will be more reliable with the larger data sample. The year-to-year variation and the multi-annual mean of the evaluated energy parameters should

*Current affiliation: Department of Atmospheric Science, University of Missouri, Columbia, Mo.

be studied from at least several years' data in studies of the large-scale atmospheric circulation. One of the big difficulties caused by confining the data coverage to a continent in the previous study was that the data represented only the area of the particular local times. By using data of more than one observation a day over the continent, we not only can overcome this difficulty, but also may obtain useful information about the diurnal variation.

With the network observations over North America, the kinetic energy budgets were studied in this paper for the 5-yr. period from May 1958 to April 1963. Twice-a-day observations were utilized, namely those at 00 and 12 GMT. Generally the 00 GMT observations correspond to late afternoon while the 12 GMT observations correspond to the very early morning for the North American Continent. The diurnal variation, seasonal change, and year-to-year fluctuations of the kinetic energy parameters are presented and discussed first for their vertical profiles, and next for their vertically integrated total budget. An attempt is then made to abstract the multi-annual mean total budget.

2. SCHEME OF COMPUTATION AND DATA

The scheme of computation is essentially the same as described in the preceding paper (Kung [11]). In the discussions to follow, \mathbf{V} is the vector of the horizontal wind, u the eastward wind component, v the northward wind component, t the time, g the acceleration of gravity, ϕ the geopotential, f the Coriolis parameter, $-\mathbf{F}$ the vector of the frictional force per unit mass, p the pressure, s the boundary of the continental region, \mathbf{n} the outward-directed unit vector normal to the continental boundary, \mathbf{k} the unit vector in the vertical direction, A the area of the continental region of the earth, ∇ the horizontal del operator along an isobaric surface, ω the vertical p -velocity, and $k = \frac{1}{2} \mathbf{V} \cdot \mathbf{V} = \frac{1}{2}(u^2 + v^2)$ the kinetic energy per unit mass. The horizontal bar denotes the area mean of a quantity over the continent. From the equation of motion

$$\frac{d\mathbf{V}}{dt} = -\nabla\phi - \mathbf{k} \times f\mathbf{V} - \mathbf{F} \quad (1)$$

or

$$\frac{\partial \mathbf{V}}{\partial t} + (\mathbf{V} \cdot \nabla)\mathbf{V} + \omega \frac{\partial \mathbf{V}}{\partial p} = -\nabla\phi - \mathbf{k} \times f\mathbf{V} - \mathbf{F}$$

and the continuity equation

$$\nabla \cdot \mathbf{V} + \frac{\partial \omega}{\partial p} = 0, \quad (2)$$

we may obtain the kinetic energy equation as the scalar product of the equation of motion and the horizontal wind vector \mathbf{V} . By integrating the kinetic energy equation over the continental area, we then get the area mean kinetic energy equation

$$-\overline{E} = -\overline{\mathbf{V} \cdot \mathbf{F}} = \frac{\partial \bar{k}}{\partial t} + \frac{1}{A} \oint_c \mathbf{V} \mathbf{k} \cdot \mathbf{n} ds + \frac{\partial \overline{\omega k}}{\partial p} + \overline{\mathbf{V} \cdot \nabla \phi} \quad (3)$$

$-\overline{\mathbf{V} \cdot \nabla \phi}$ in equation (3) is the generation or, more specifically, the generation of kinetic energy by the work done by the horizontal pressure force. This term may be expressed as

$$-\overline{\mathbf{V} \cdot \nabla \phi} = -\overline{\nabla \cdot \mathbf{V} \phi} - \frac{\partial \overline{\omega \phi}}{\partial p} - \overline{\omega \alpha} \quad (4)$$

where α is the specific volume of the air. The process represented by $-\overline{\omega \alpha}$ may be regarded as the release of available potential energy, while $-\overline{\nabla \cdot \mathbf{V} \phi}$ and $-\partial \overline{\omega \phi} / \partial p$ may be regarded as the redistribution terms required for the released energy finally to appear as the actual generation of the kinetic energy which is measured by $-\overline{\mathbf{V} \cdot \nabla \phi}$. If equation (4) is integrated over the entire mass of the atmosphere, M , it becomes

$$-\int_M \overline{\mathbf{V} \cdot \nabla \phi} dM = -\int_M \overline{\omega \alpha} dM \quad (5)$$

and $-\overline{\omega \alpha}$ may be used instead of $-\overline{\mathbf{V} \cdot \nabla \phi}$ for the global or hemispherical estimation of the kinetic energy generation. Although some confusion in nomenclature exists, we shall call $-\overline{\mathbf{V} \cdot \nabla \phi}$ the energy generation and $-\overline{\omega \alpha}$ the energy conversion throughout this paper. In this study a direct estimate of $-\overline{\mathbf{V} \cdot \nabla \phi}$ rather than $-\overline{\omega \alpha}$ was made from observed wind and geopotential data. In this way we can avoid controversies in estimating ω , and also can obtain the dissipation \overline{E} as the residual of the energy equation (3) without further need for estimation of $-\overline{\nabla \cdot \mathbf{V} \phi}$ and $-\partial \overline{\omega \phi} / \partial p$. The evaluation of $-\overline{\mathbf{V} \cdot \nabla \phi}$, which essentially depends on the ageostrophic component of the observed wind, is the key to the present series of studies; for the technique of computation, reference may be made to previous papers (Kung [10, 11]).

Other energy parameters in equation (3) to be computed along with the generation $-\overline{\mathbf{V} \cdot \nabla \phi}$ are the local change $\partial \bar{k} / \partial t$, the horizontal outflow $(1/A) \oint_c \mathbf{V} \mathbf{k} \cdot \mathbf{n} ds$ ($= \overline{\nabla \cdot \mathbf{V} k}$), the vertical transport $\partial \overline{\omega k} / \partial p$, and the dissipation \overline{E} ($= \overline{\mathbf{V} \cdot \mathbf{F}}$) as the residual term.

By making use of the continuity equation (2), we may kinematically obtain the vertical p -velocity ω as

$$\omega_{p_1} = \int_{p_1}^{p_2} \nabla \cdot \mathbf{V} dp + \omega_{p_2} \quad (6)$$

where ω_{p_1} and ω_{p_2} are ω at pressure levels p_1 and p_2 . From this the area mean $\bar{\omega}$ was computed by

$$\bar{\omega}_{p_1} = \frac{1}{A} \int_{p_1}^{p_2} \oint_c \mathbf{V} \cdot \mathbf{n} ds dp + \bar{\omega}_{p_2} \quad (7)$$

with an assumption that $\bar{\omega} = 0$ at the surface level.

We note that errors in estimating the wind divergence should decrease in proportion to the characteristic length-scale of the domain of analysis; that, for our domain of analysis, $\overline{\omega k}$ might contribute significantly to $\overline{\omega k}$; and that in the large-scale kinetic energy budget, the vertical transport term $\partial \overline{\omega k} / \partial p$ is small in magnitude as evidenced in various studies (e.g., Holopainen [7], Jensen [8], and Smagorinsky, Manabe, and Holloway [18]). For these reasons $\overline{\omega k}$ is substituted for $\overline{\omega k}$ in evaluating $\partial \overline{\omega k} / \partial p$. To test this substitution, we note that $\partial \overline{\omega k} / \partial p$ should vanish after integration from the surface to the top of the atmosphere, or should be negligibly small after integration from the surface to a very high level of the atmosphere. Indeed, as shown in table 4 of this paper and in the preceding paper (Kung [11]), $\partial \overline{\omega k} / \partial p = \partial \overline{\omega k} / \partial p$, integrated from the surface to 50 mb., almost vanishes in the summer and becomes negligibly small in the winter for the balance of the energy parameters.

The twice-a-day wind and geopotential observations at 00 and 12 GMT over the North American Continent and some surrounding regions for a 5-yr. period from May 1958 to April 1963 were obtained from the MIT General Circulation Data Library (The National Science Foundation Grant GP 820 and GP 3657). All 5 years' data were utilized for the 00 GMT observations. However, because of a technical difficulty with the data tapes in our possession, 3 months' data (January and September 1959, and April 1962) were not utilized for the 12 GMT observations.

The continental area of the data coverage included the continental United States, Alaska, and Canada (see Kung [10, 11] for the location of stations). There were a total of 101 stations on or within the continental boundary, constituting a uniform and dense aerological network. An additional 18 stations located outside the continental boundary were also used to assist in the estimation of $\nabla \phi$ and data editing. The computation was carried out separately for 00 and 12 GMT data on a daily basis for each of the 20 pressure layers from the surface to 50 mb. The computation from the surface to 100 mb. was made for the entire 5-yr. period. However, as a result of the rather sparse data above the 100-mb. level in the earlier years, the computations for the uppermost two layers (100–70 mb. and 70–50 mb.) were done only for the latest 2- or 3-yr. period. This is to be understood throughout this paper in discussion of the 5-yr. mean values. $\nabla \phi$ at the surface was computed from the geopotential height of the 1000-mb. level. Occasionally there are days with relatively few available stations, and they were eliminated during the analysis; data for the first day of each month were used only to compute $\partial \overline{k} / \partial t$ for the next day. Since the number of those unavailable days is very small for each month, no special effort was made to correct for the effect of the unavailable days. A monthly value of an energy parameter for 00 or 12 GMT observations was obtained by averaging the computed daily values at 00 or 12 GMT separately. These monthly values were further averaged to obtain seasonal mean or multi-annual mean values.

It should be noted that over North America, the coverage of aerological data from the MIT Data Library was fairly dense even to the high altitudes. For an analysis of the quality of the utilized data, reference may be made to Kung [11] and The Travelers Research Center, Inc. [20].

3. VERTICAL PROFILE OF ENERGY PARAMETERS

Vertical profiles of the kinetic energy generation $-\overline{\mathbf{V} \cdot \nabla \phi}$ based on averages from daily values during the 5-yr. period are shown separately for 00 and 12 GMT observations in figure 1 for the winter 6 months (October through March), for the summer 6 months (April through September), and for the annual mean.

As the computation of the energy generation, $-\overline{\mathbf{V} \cdot \nabla \phi}$ essentially depends on the ageostrophic component of the observed wind, we may expect a considerable diurnal variation of $-\overline{\mathbf{V} \cdot \nabla \phi}$ when there is a significant diurnal variation of the wind. Rasmusson [14], in his water vapor budget study over North America, recognized a highly ageostrophic character in the diurnal oscillations in the hodographs of the lower and middle troposphere, and predicted the corresponding variations in $-\overline{\mathbf{V} \cdot \nabla \phi}$.

As is clearly shown in figure 1, the diurnal variation of the generation term is very significant, not only in the lower and middle troposphere but notably at the jet stream level. More kinetic energy is generated in the lower troposphere and at the jet stream level at 00 GMT than at 12 GMT, and less in the middle troposphere at 00 GMT than at 12 GMT. The larger generation value at 00 GMT in the lower troposphere and at the jet stream level is especially pronounced during the summer, even changing the sign of $-\overline{\mathbf{V} \cdot \nabla \phi}$ above the 270-mb. level. Smagorinsky, Manabe, and Holloway [18], in their nine-level model numerical experiment of the general circulation, showed that there were two maxima of $-\overline{\mathbf{V} \cdot \nabla \phi}$; one in the lower troposphere, and one at the jet stream level, while $-\overline{\omega \alpha}$ is at its maximum in the middle troposphere. Though $-\overline{\omega \alpha}$ is not computed in this study, we may expect a larger value of $-\overline{\omega \alpha}$ at 00 GMT than at 12 GMT in the middle troposphere.

00 GMT generally means the late afternoon, and 12 GMT the very early morning on the North American Continent. Considering the domain of analysis in this study, there is a possibility that organized large-scale variations of the vertical motion and divergence patterns resulting from the surface heating are the cause of the significant diurnal variation of the $-\overline{\mathbf{V} \cdot \nabla \phi}$ profile. Some observational studies seem to support this point. Curtis and Panofsky [2] carefully studied the mean large-scale vertical motion over the midwestern United States for a 10-day period in July, and indicated a significant diurnal variation. Bleeker and Andre [1] also studied about the same area for August, and found important diurnal variations in the mean divergence field. More recently Hering and Borden [6] revealed prominent features of the diurnal wind

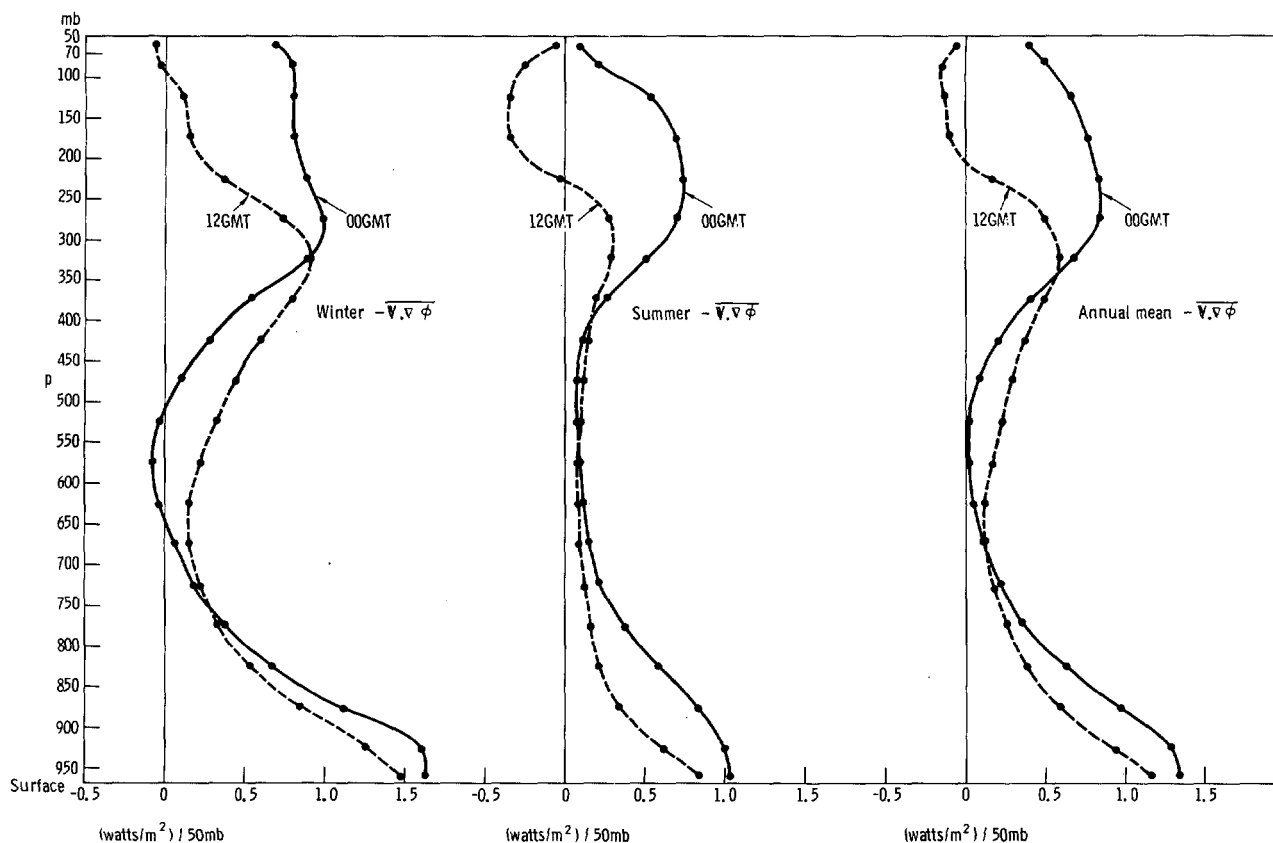


FIGURE 1.—Vertical profile of the kinetic energy generation $-\overline{V \cdot \nabla \phi}$ at 00 and 12 GMT for the 5-yr. period.

variation over the central United States in July 1958. They defined three well-organized oscillation regimes, showing maximum amplitudes of diurnal variation in wind components at 0.6-, 5-, and 12-km. heights. However, their finding of the diurnal wind oscillations might indicate other aspects of the tidal oscillation as well as the vertical motion directly induced by the diurnal surface heating. It is noteworthy that the 12-km. height roughly corresponds to the 200-mb. level, about where we have the maximum diurnal variation of $-\overline{V \cdot \nabla \phi}$ profile during the summer. In addition to the organized large-scale diurnal variation of the wind pattern caused by the surface heating, however, we also should not exclude the possibility of the contribution to the diurnal variation of $-\overline{V \cdot \nabla \phi}$ from certain diurnal wind variations of this nature in a more local scale, related to complex land-sea breeze systems, mountain-valley wind systems, etc.

In discussing the diurnal variations of the generation term $-\overline{V \cdot \nabla \phi}$, the nature of the atmospheric tidal oscillation should be given attention. The analyses of Finger, Harris, and Teweles [4] and Harris, Finger, and Teweles [5] suggest that there are distinct amplitudes and phases for the diurnal and semidiurnal tidal oscillations of the observed isobaric height and wind components. As the value of $-\overline{V \cdot \nabla \phi}$ depends sensitively on the ageostrophic components of the observed wind, the small amplitudes

of oscillation in the observed height and wind, together with their phase differences in oscillation, might have a significant effect on the computed diurnal variation of the $-\overline{V \cdot \nabla \phi}$.

The possible effect of the radiation error in the radiosonde observations on the computation of $-\overline{V \cdot \nabla \phi}$ in the upper part of the atmosphere also should not be excluded from the discussion of the computed diurnal variations. This effect is supposedly more significant in the summer than in the winter. No correction for the observational data was attempted in this study. Wind observations are not known to have systematic errors (see Finger, Harris, and Teweles [4]). The systematic radiation errors in reported heights may be canceled in the process of computing the gradient of geopotential, and the computed vertical profile of $-\overline{V \cdot \nabla \phi}$ converges to zero in the stratosphere in the summer. Thus a reasonable reliability may be assumed in the computed results. However, this is an open question at this stage.

The corresponding vertical profiles of the dissipation term for the 5-yr. period are also shown separately for 00 and 12 GMT observations in figure 2. The dissipation \overline{E} is significantly larger in the lower troposphere and at the jet stream level at 00 GMT than at 12 GMT. This diurnal variation is also most pronounced in the summer. In regard to the negative dissipation value at 12 GMT above the maxi-

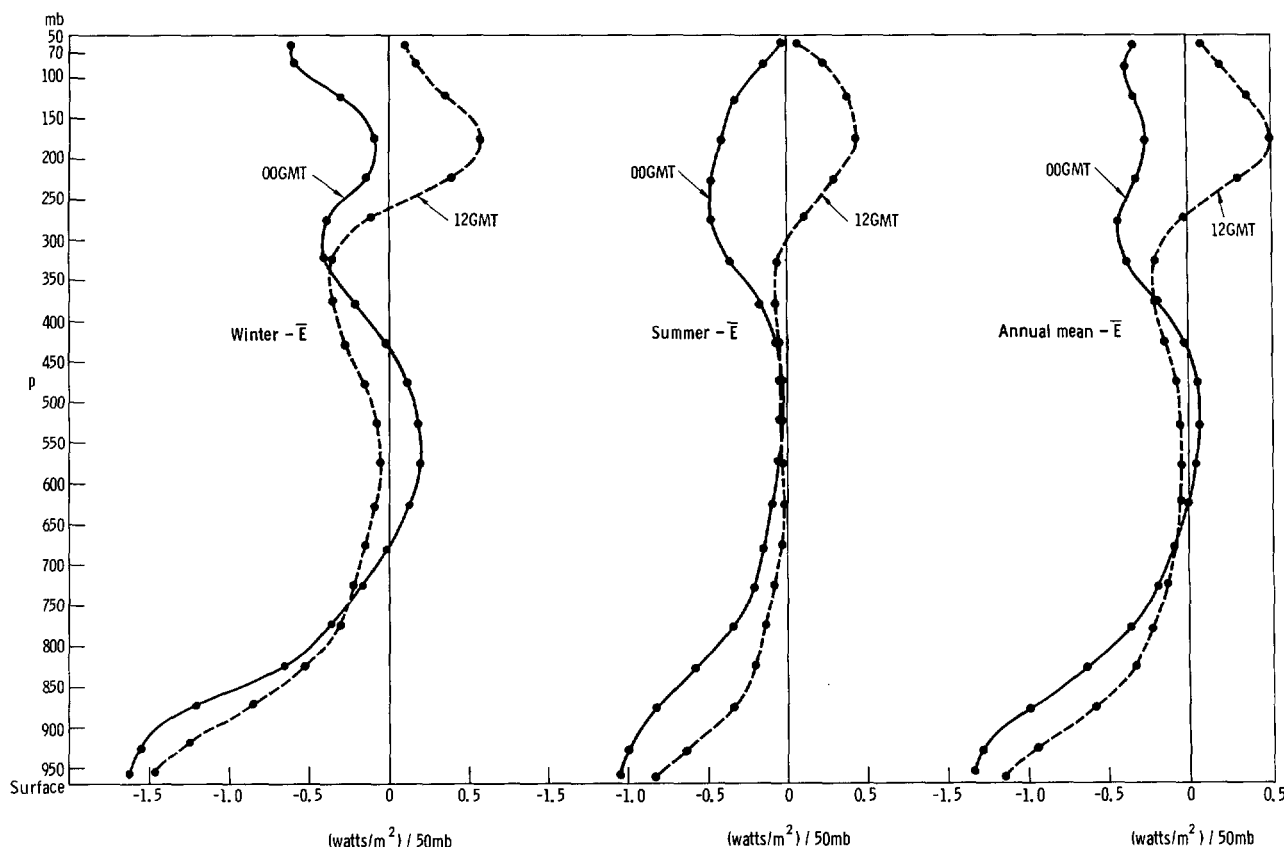


FIGURE 2.—Vertical profile of the kinetic energy dissipation \bar{E} at 00 and 12 GMT for the 5-yr. period.

imum jet stream level, we should note that the dissipation \bar{E} presented in this paper is the dissipation observed with the existing network of rawinsonde/radiosonde observations, and that \bar{E} was obtained as the residual term to balance other energy parameters, mainly the generation $-\bar{\mathbf{V}} \cdot \nabla \phi$ and horizontal outflow $(1/A) \oint_c \mathbf{V} \cdot \mathbf{k} \cdot \mathbf{n} ds$, in the kinetic energy equation. Thus either undetected eddies at 12 GMT with the density of the observational network at that altitude, and/or systematic overestimate of the outflow term may lead to negative \bar{E} values. Some possibility of underestimation of the dissipation \bar{E} above the jet core level may be mentioned in this respect. It also must be noted that estimate of the local change $\partial \bar{k} / \partial t$ was based on the observations 24 hr. apart, introducing a possibility of a bias in estimating the dissipation \bar{E} .

Figures 3 and 4 respectively show the vertical profiles of the generation $-\bar{\mathbf{V}} \cdot \nabla \phi$ and dissipation \bar{E} averaged from 00 and 12 GMT observations for the winter, summer, and multi-annual mean. The vertical profiles confirm the previous study (Kung [11]) with 00 GMT observations for 11 months: the generation and dissipation are at a maximum in the planetary boundary layer, they decrease gradually to a minimum in the middle troposphere, increase again to the second maximum at the jet stream

level, and then decrease again farther upward. The general shapes of the vertical profiles of the generation and dissipation predicted in the numerical experiment by Smagorinsky, Manabe, and Holloway [18] are actually closer to those presented in this paper than to those in the previous paper. However, the proportion of the dissipation at the jet stream level in their numerical experiment seems to be larger than that indicated in this study.

As mentioned in the introduction of this paper, by using data of more than one observation per day we may expect results of the regional study over the continent to be closer to those that would be obtained for an entire hemisphere. However, a simple average of the 00 and 12 GMT results may not be sufficient in this respect if the presence of the higher harmonics significantly influences the computed energy parameters. Harris, Finger, and Teweles [5] showed in their study of the atmospheric tide, that the semidiurnal variation of the observed height and wind might be as important as the diurnal variations for the portion of the atmosphere we are investigating.

The vertical distribution of the kinetic energy budget averaged for 00 and 12 GMT is shown for the winter in table 1, for the summer in table 2, and for the multi-annual mean in table 3. Inspection of these tables should indicate a balance of the energy parameters as required by equation (3):

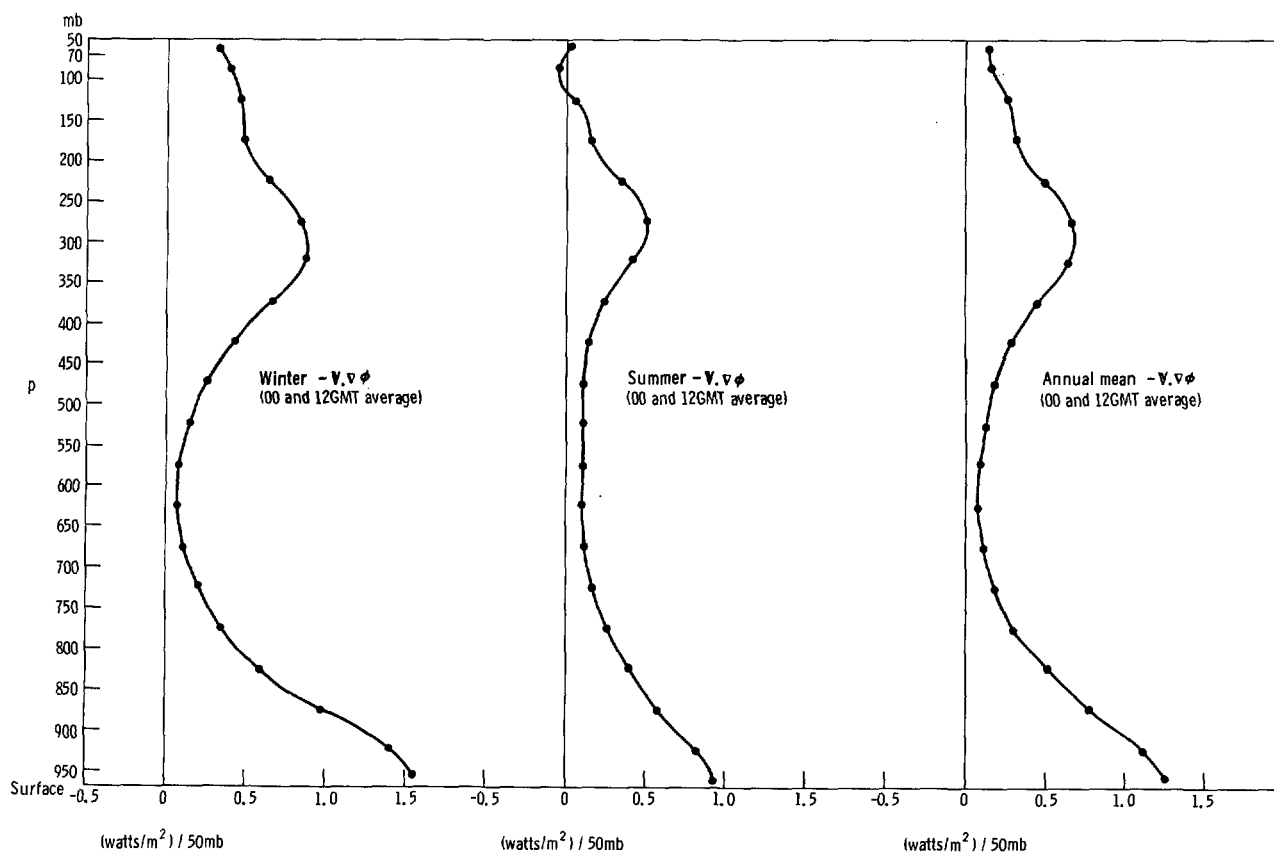


FIGURE 3.—Vertical profile of the kinetic energy generation $-\overline{\mathbf{V} \cdot \nabla \phi}$ for the 5-yr. period (average of 00 and 12 GMT).

TABLE 1.—Winter mean kinetic energy budget within each pressure layer during the 5-yr. period with 00 and 12 GMT data (October, November, December, January, February, and March). \bar{k} is in units of 10^5 joules/m². Other quantities are in watts/m².

| Pressure layer (mb.) | \bar{k} | $\frac{\partial \bar{k}}{\partial t}$ | $\frac{1}{A} \oint_c \mathbf{V} \cdot \mathbf{k}_{nds}$ | $\frac{\partial \omega \bar{k}}{\partial p}$ | $-\overline{\mathbf{V} \cdot \nabla \phi}$ | \bar{E} |
|----------------------|-----------|---------------------------------------|---|--|--|-----------|
| 969*-950 | 0.051 | -0.001 | 0.006 | -0.004 | 0.602 | 0.601 |
| 950-900 | .226 | .002 | .018 | -.010 | 1.420 | 1.415 |
| 900-850 | .283 | -.002 | .015 | -.009 | .980 | .976 |
| 850-800 | .328 | -.001 | .013 | -.004 | .599 | .592 |
| 800-750 | .379 | -.001 | .017 | -.005 | .358 | .346 |
| 750-700 | .457 | -.001 | .030 | -.006 | .217 | .194 |
| 700-650 | .563 | .001 | .061 | -.008 | .124 | .069 |
| 650-600 | .698 | .004 | .104 | -.011 | .074 | -.023 |
| 600-550 | .859 | .003 | .154 | -.016 | .082 | -.059 |
| 550-500 | 1.055 | .003 | .210 | -.016 | .149 | -.048 |
| 500-450 | 1.289 | .003 | .273 | -.020 | .266 | .011 |
| 450-400 | 1.568 | .001 | .336 | -.031 | .435 | .129 |
| 400-350 | 1.893 | -.002 | .406 | -.023 | .665 | .284 |
| 350-300 | 2.228 | .001 | .496 | -.027 | .860 | .391 |
| 300-250 | 2.462 | -.002 | .655 | -.050 | .850 | .247 |
| 250-200 | 2.428 | -.004 | .853 | -.074 | .635 | -.141 |
| 200-150 | 2.030 | -.001 | .777 | -.038 | .488 | -.251 |
| 150-100 | 1.408 | -.002 | .444 | .055 | .469 | -.027 |
| 100-70 | .570 | -.001 | .100 | .009 | .234 | .126 |
| 70-50 | .297 | -.001 | .055 | -.028 | .129 | .103 |

*Area mean surface pressure.

TABLE 2.—Summer mean kinetic energy budget within each pressure layer during the 5-yr. period with 00 and 12 GMT data (April, May, June, July, August, and September). \bar{k} is in units of 10^5 joules/m². Other quantities are in watts/m².

| Pressure layer (mb.) | \bar{k} | $\frac{\partial \bar{k}}{\partial t}$ | $\frac{1}{A} \oint_c \mathbf{V} \cdot \mathbf{k}_{nds}$ | $\frac{\partial \omega \bar{k}}{\partial p}$ | $-\overline{\mathbf{V} \cdot \nabla \phi}$ | \bar{E} |
|----------------------|-----------|---------------------------------------|---|--|--|-----------|
| 967*-950 | 0.038 | 0.000 | -0.004 | .003 | 0.321 | 0.321 |
| 950-900 | .171 | -.000 | -.006 | .010 | .813 | .809 |
| 900-850 | .200 | -.000 | .003 | .007 | .584 | .575 |
| 850-800 | .217 | -.000 | .010 | .005 | .401 | .387 |
| 800-750 | .240 | -.001 | .019 | .006 | .270 | .246 |
| 750-700 | .279 | -.001 | .023 | .007 | .182 | .152 |
| 700-650 | .334 | -.002 | .028 | .009 | .131 | .095 |
| 650-600 | .406 | -.002 | .039 | .009 | .111 | .065 |
| 600-550 | .494 | -.001 | .055 | .011 | .103 | .038 |
| 550-500 | .599 | -.002 | .064 | .009 | .099 | .027 |
| 500-450 | .727 | -.002 | .070 | .013 | .109 | .028 |
| 450-400 | .889 | -.002 | .087 | .012 | .131 | .035 |
| 400-350 | 1.090 | -.003 | .116 | .012 | .229 | .104 |
| 350-300 | 1.318 | -.003 | .199 | -.007 | .402 | .212 |
| 300-250 | 1.523 | -.003 | .315 | -.034 | .500 | .222 |
| 250-200 | 1.545 | -.002 | .351 | -.057 | .365 | .073 |
| 200-150 | 1.206 | -.000 | .238 | -.032 | .167 | -.039 |
| 150-100 | .647 | -.001 | .089 | .005 | .081 | -.013 |
| 100-70 | .156 | -.001 | .013 | -.003 | -.025 | -.034 |
| 70-50 | .057 | -.000 | .004 | .000 | .009 | .005 |

*Area mean surface pressure.

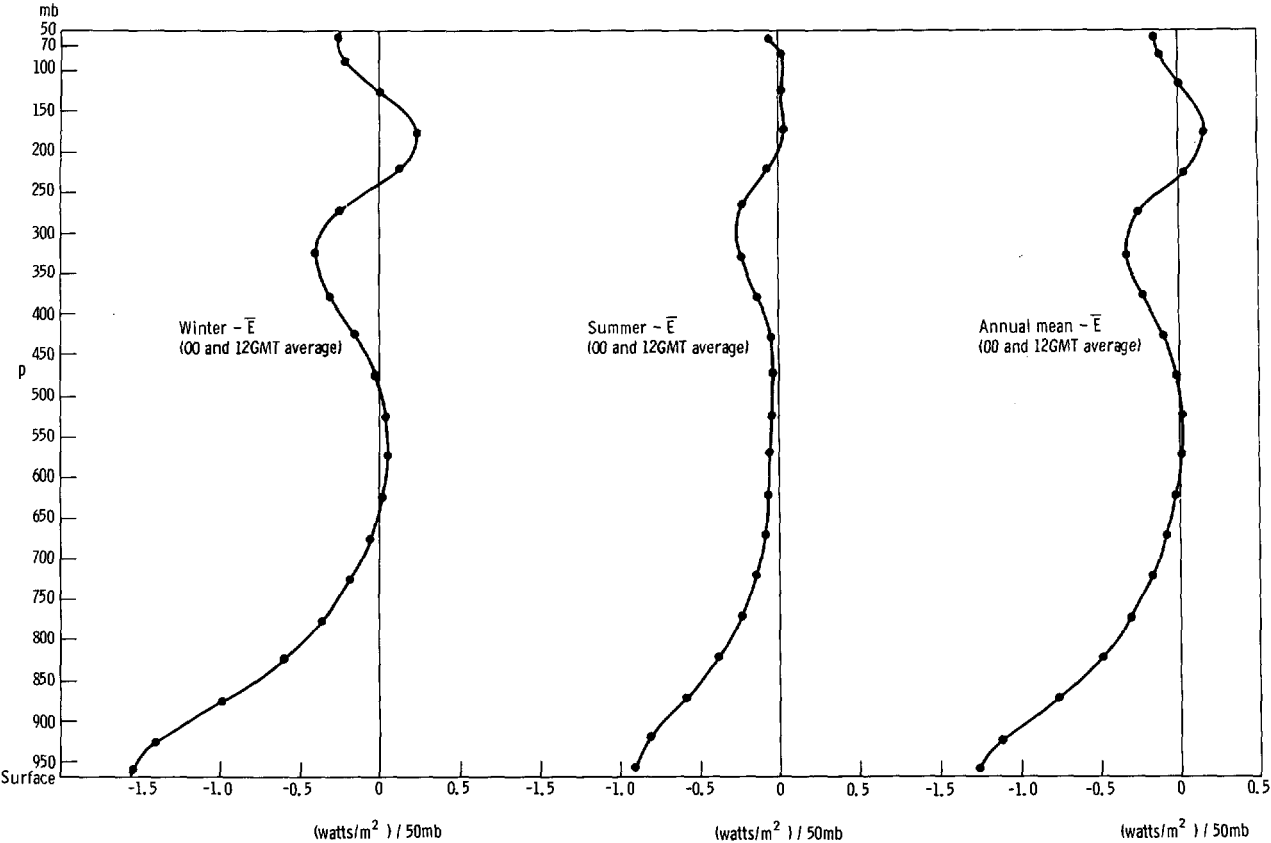


FIGURE 4.—Vertical profile of the kinetic energy dissipation \bar{E} for the 5-yr. period (average of 00 and 12 GMT).

$$\bar{E} = -\frac{\partial \bar{k}}{\partial t} - \frac{1}{A} \oint_c \mathbf{V}k \cdot \mathbf{n}ds - \frac{\partial \bar{\omega}k}{\partial p} - \mathbf{V} \cdot \nabla \phi.$$

TABLE 3.—Multi-annual mean kinetic energy budget within each pressure layer during the 5-yr. period with 00 and 12 GMT data. k is in units of 10^5 joules/ m^2 . Other quantities in watts/ m^2 .

| Pressure layer (mb.) | \bar{k} | $\frac{\partial \bar{k}}{\partial t}$ | $\frac{1}{A} \oint_c \mathbf{V}k \cdot \mathbf{n}ds$ | $\frac{\partial \bar{\omega}k}{\partial p}$ | $-\mathbf{V} \cdot \nabla \phi$ | \bar{E} |
|----------------------|-----------|---------------------------------------|--|---|---------------------------------|-----------|
| 968*-950 | 0.044 | -.000 | 0.001 | -0.000 | 0.461 | 0.461 |
| 950-900 | .199 | -.001 | .006 | .000 | 1.117 | 1.112 |
| 900-850 | .242 | -.001 | .009 | -.001 | .782 | .775 |
| 850-800 | .272 | -.001 | .011 | .000 | .500 | .489 |
| 800-750 | .309 | -.001 | .018 | .000 | .314 | .296 |
| 750-700 | .368 | -.001 | .027 | .000 | .199 | .173 |
| 700-650 | .449 | -.000 | .045 | .001 | .127 | .082 |
| 650-600 | .552 | .001 | .071 | -.001 | .093 | .021 |
| 600-550 | .676 | .001 | .104 | -.002 | .092 | -.011 |
| 550-500 | .827 | .000 | .137 | -.003 | .124 | -.010 |
| 500-450 | 1.008 | .000 | .171 | -.003 | .187 | .019 |
| 450-400 | 1.228 | -.001 | .211 | -.010 | .283 | .082 |
| 400-350 | 1.492 | -.002 | .261 | -.005 | .447 | .194 |
| 350-300 | 1.773 | -.001 | .348 | -.017 | .631 | .302 |
| 300-250 | 1.993 | -.032 | .485 | -.042 | .675 | .234 |
| 250-200 | 1.986 | -.003 | .602 | -.065 | .500 | -.034 |
| 200-150 | 1.618 | -.000 | .508 | -.035 | .328 | -.145 |
| 150-100 | 1.028 | -.001 | .267 | .030 | .275 | -.020 |
| 100-70 | .363 | -.001 | .056 | .003 | .105 | .046 |
| 70-50 | .177 | -.000 | .029 | -.014 | .069 | .054 |

*Area mean surface pressure.

The multi-annual mean kinetic energy balance is plotted in figure 5, except for the local change $\partial \bar{k} / \partial t$ which is entirely negligible in magnitude. As the magnitude of the vertical transport $\partial \bar{\omega} k / \partial t$ is very small, approximate balance of the generation $-\mathbf{V} \cdot \nabla \phi$, horizontal outflow $(1/A) \oint_c \mathbf{V}k \cdot \mathbf{n}ds$, and dissipation \bar{E} exists. In the lower troposphere we observe approximate balance of the generation and dissipation. The significantly large horizontal outflow at the jet stream level implies that the kinetic energy which is generated over North America and transported to the North Atlantic must be dissipated beyond the continental boundary.

The march of the seasons is depicted in the monthly variation of the vertical distribution of the generation $-\mathbf{V} \cdot \nabla \phi$ and dissipation \bar{E} for the 5-yr. period in the pressure-time cross sections in figures 6 and 7. The numerical values are averages of the 00 and 12 GMT observations. The general features of the vertical distributions of $-\mathbf{V} \cdot \nabla \phi$ and \bar{E} are essentially the same as presented by the vertical profiles for the winter and sum-

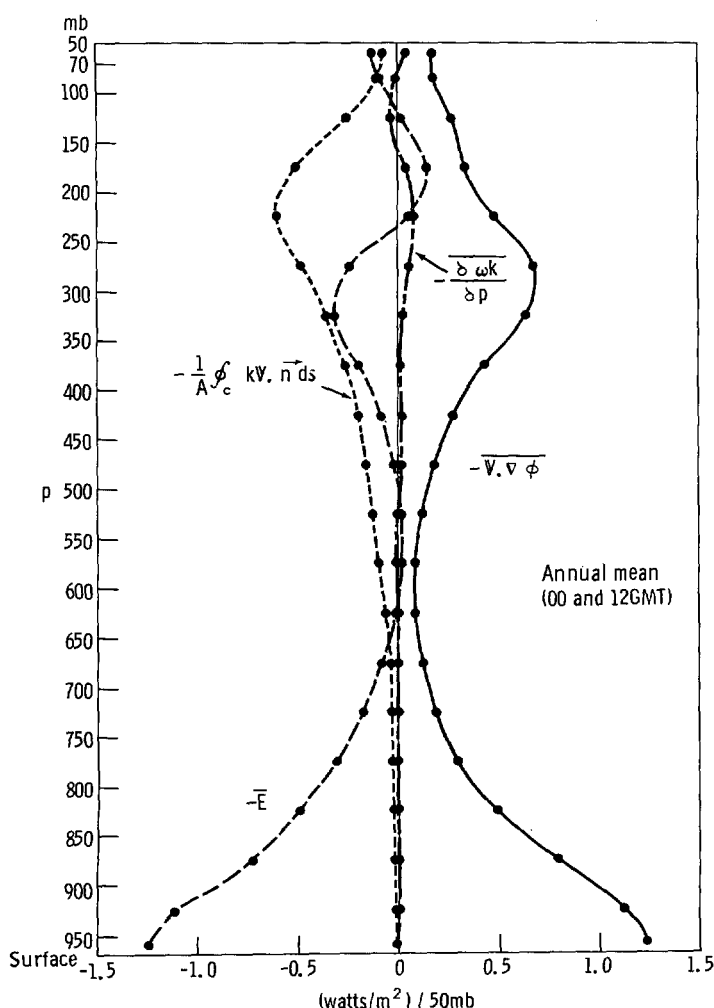


FIGURE 5.—Multi-annual mean vertical profile of the kinetic energy balance for the 5-yr. period (average of 00 and 12 GMT).

mer 6 months in figures 3 and 4. Generally the generation and dissipation are stronger in winter than in summer, although the feature of the maxima of $-\bar{\mathbf{V}} \cdot \nabla \phi$ and \bar{E} both in the planetary boundary layer and at the jet stream level is clearly observed throughout the year. The negative $-\bar{\mathbf{V}} \cdot \nabla \phi$ in the lower stratosphere in the late spring and fall, previously shown (Kung [11]) for a 1-yr. period, is still observed in this 5-yr. average.

While the mean vertical profiles of the energy parameters for the 5-yr. period have been discussed above, we may expect considerable variations in a long time series. Monthly mean profiles of $-\bar{\mathbf{V}} \cdot \nabla \phi$ and \bar{E} of February and August are plotted separately for the individual 5 years for the average of 00 and 12 GMT observations in figures 8 and 9. There is a significant variation in the magnitude of these quantities as represented by individual profiles (also see figs. 10 and 12 in this connection). However, the basic features of the profiles with two maxima in the boundary layer and at the jet stream level remain the same for individual cases.

This is not only true for the examples shown in figures 8 and 9, but it is also true for most of the individual months and days in the 5-yr. period.

4. VERTICALLY INTEGRATED ENERGY PARAMETERS

Monthly means of the vertically integrated total energy parameters from the surface to 100 mb., including the kinetic energy level \bar{k} , the generation $-\bar{\mathbf{V}} \cdot \nabla \phi$, the horizontal outflow $(1/A) \oint \mathbf{V} \mathbf{k} \cdot \mathbf{n} ds$, and the dissipation \bar{E} are plotted separately for 00 and 12 GMT observations for the 60 months during the 5-yr. period in figure 10, except for unavailable 12 GMT observations of January and September 1959, and April 1962. Figure 11 is the corresponding monthly variation of the vertically integrated energy parameters averaged for the 5-yr. period. As shown in these figures, and also as evidenced in the vertical profiles in figures 1 and 2, the vertically integrated generation $-\bar{\mathbf{V}} \cdot \nabla \phi$ and the dissipation \bar{E} required for balance are both significantly and consistently higher at 00 GMT than at 12 GMT in the summer. This diurnal variation is also most pronounced during the mid-summer months. The monthly kinetic energy level \bar{k} reaches a rather sharp peak during the winter, especially in January 1962 and 1963, and the generation $-\bar{\mathbf{V}} \cdot \nabla \phi$ and horizontal outflow $(1/A) \oint \mathbf{V} \mathbf{k} \cdot \mathbf{n} ds$ are correspondingly at their peak during the same period. The annual cycle of the energy parameters in terms of month-to-month variation of the plotted energy parameter (fig. 11) seems to reflect the march of the seasons in a very pronounced way.

The year-to-year variation of the atmospheric energy is an interesting phenomenon. Krueger, Winston, and Haines [9] investigated the yearly differences of the energy level in the zonal and eddy components of the available potential and kinetic energy, and also the differences of the conversion between zonal and eddy available potential energy for an approximately corresponding 5-yr. period, and found them very significant, particularly in winter.

The year-to-year variation of the vertically integrated total kinetic energy parameters in this study is shown in figure 12, as indicated by the annual mean values of each year from May to the next April. While the year-to-year variation of the generation $-\bar{\mathbf{V}} \cdot \nabla \phi$ and dissipation \bar{E} is significant, the differences between 00 and 12 GMT are nearly constant from year to year: 3.72 watts/m.² for $-\bar{\mathbf{V}} \cdot \nabla \phi$ and 4.00 watts/m.² for \bar{E} are the average differences between the twice-daily observations. This is a rather remarkable feature in the time series of energy parameters, and the diurnal variation should be regarded as one of the prominent components in the fundamental time oscillation of atmospheric energy. On the other hand, the significant year-to-year variation of $-\bar{\mathbf{V}} \cdot \nabla \phi$ and \bar{E} points out that the energy budget study with a short-

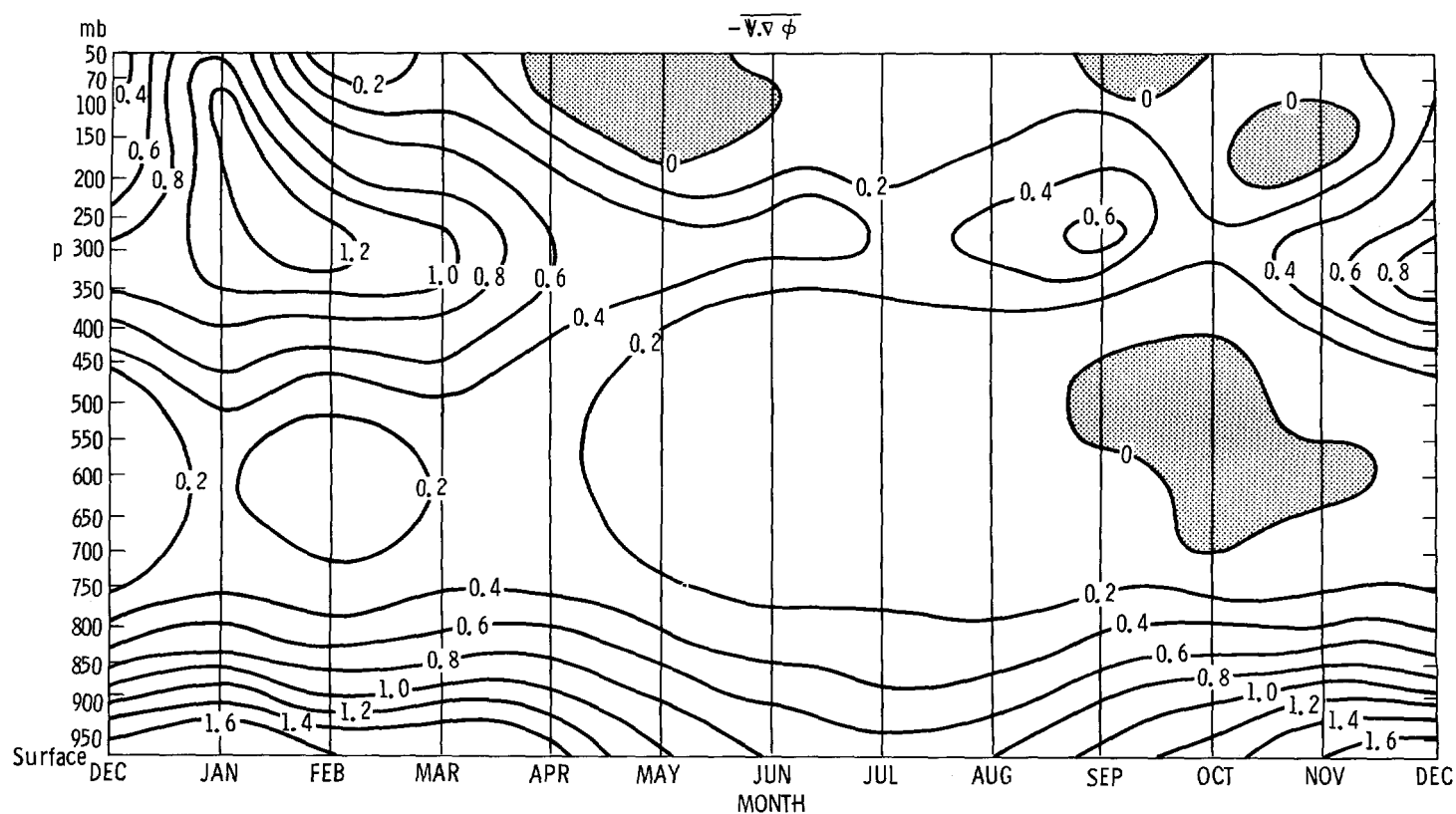


FIGURE 6.—Pressure-time cross section of mean monthly kinetic energy generation $-\mathbf{V} \cdot \nabla \phi$ for the 5-yr. period. Values are averaged for 00 and 12 GMT and in units of $(\text{watts/m}^2)/50 \text{ mb}$.

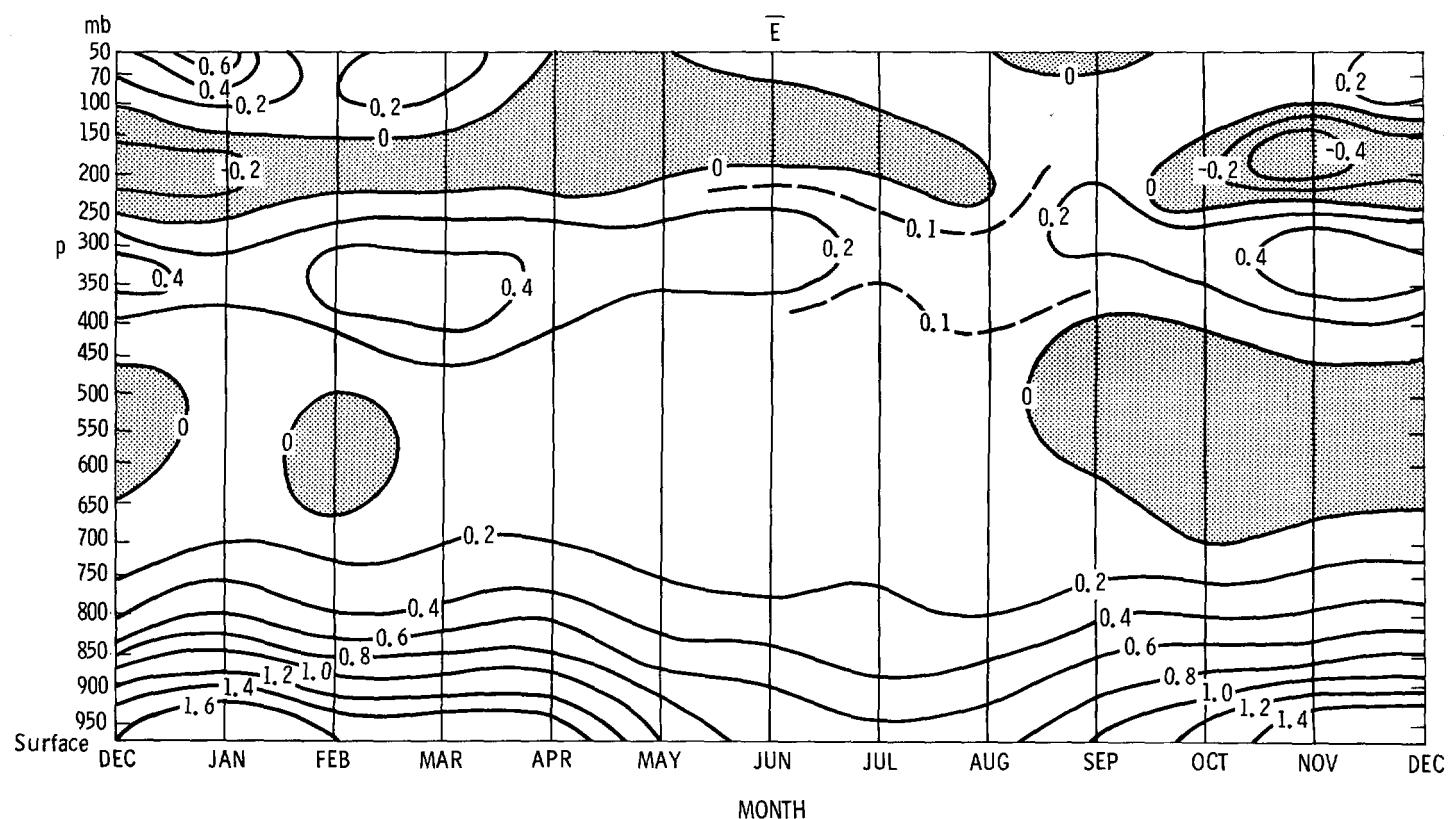


FIGURE 7.—Pressure-time cross sections of mean monthly kinetic energy dissipation \bar{E} for the 5-yr. period. Values are averaged for 00 and 12 GMT in units of $(\text{watts/m}^2)/50 \text{ mb}$.

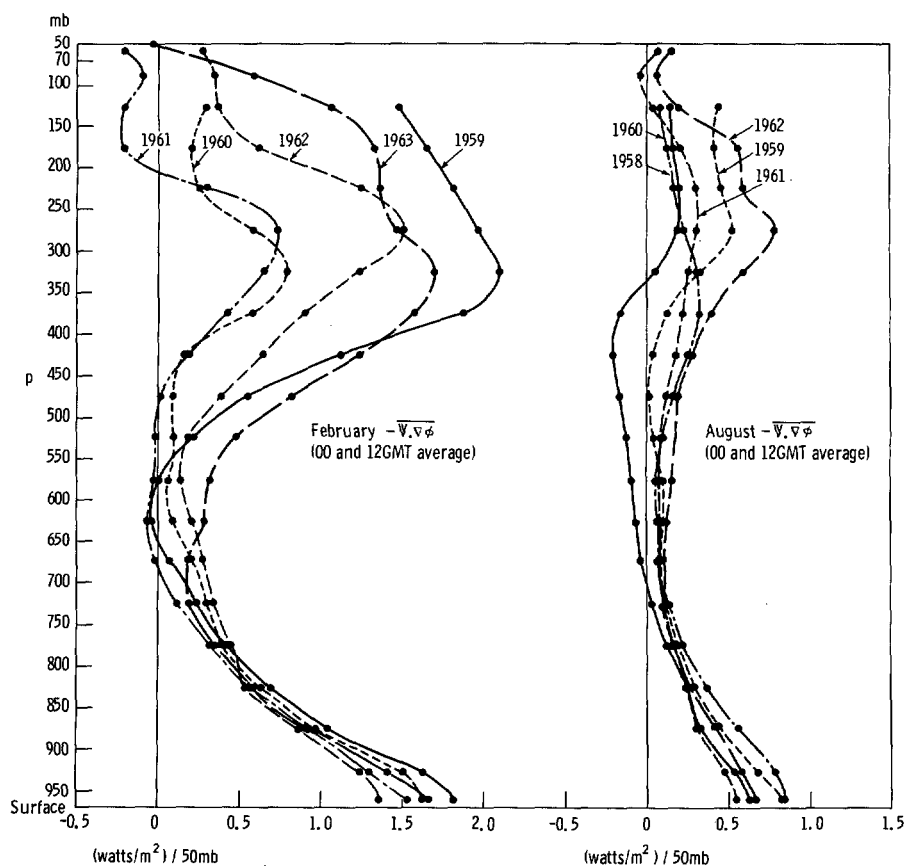


FIGURE 8.—Yearly variation of the February and August kinetic energy generation $-\bar{\mathbf{V}} \cdot \nabla \phi$ (00 and 12 GMT average).

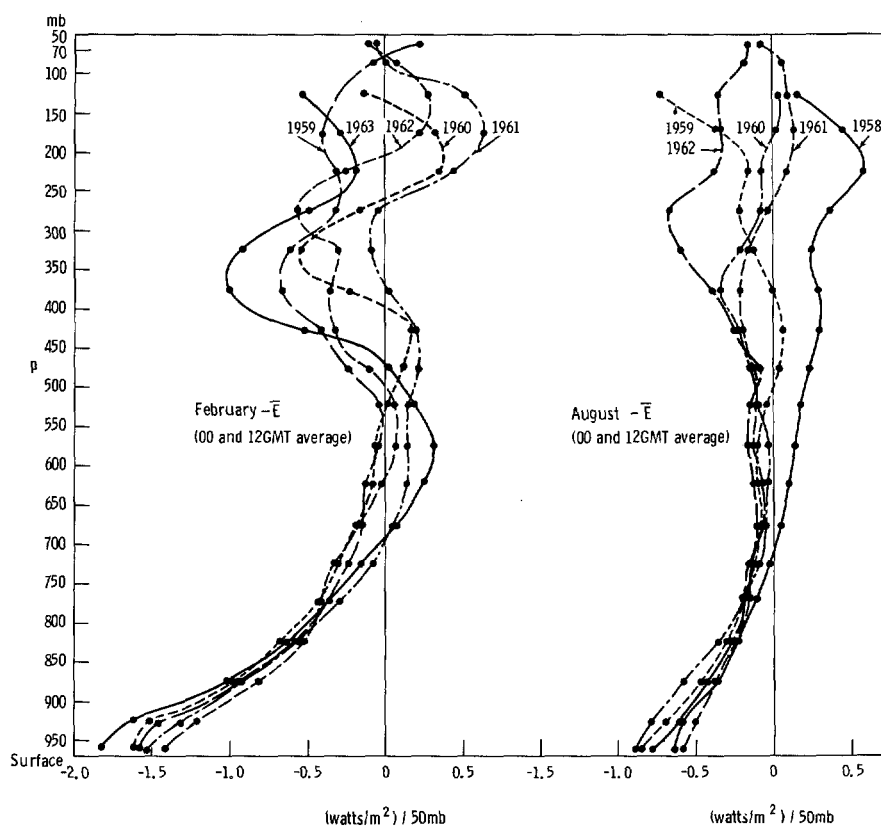


FIGURE 9.—Yearly variation of the February and August kinetic energy dissipation \bar{E} (00 and 12 GMT average).

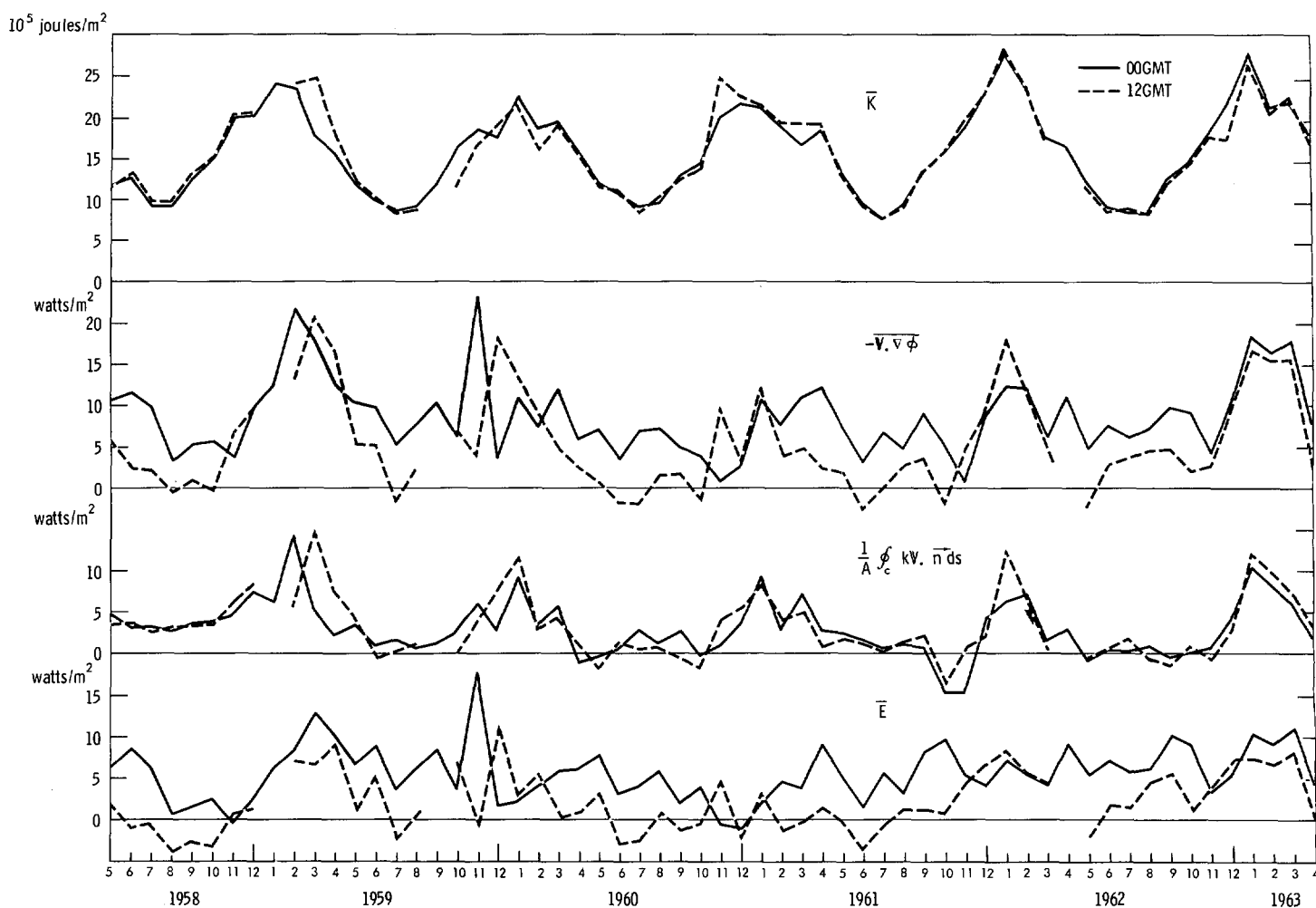


FIGURE 10.—Monthly variation of the vertically integrated kinetic energy parameters from May 1958 through April 1963. \bar{k} energy level, $-\bar{\mathbf{V}} \cdot \nabla \phi$ generation, $(1/A) \oint \mathbf{V}_k \cdot \mathbf{n} ds$ horizontal outflow, and \bar{E} dissipation.

period data sample is of limited value in discussion of the multi-annual mean values. In this specific respect the data sample should be at least the length (5 yr.) of that used in the present study.

5. MULTI-ANNUAL MEAN ENERGY BUDGET

The multi-annual mean total kinetic energy budget, which is integrated from the surface to the 50-mb. level, is summarized in table 4. The table compares the 00 GMT energy budget with the 12 GMT budget for the winter, summer, and annual mean.

The kinetic energy level \bar{k} does not show a significant diurnal variation for 00 and 12 GMT. Values of \bar{k} for summer, winter, and on an annual basis are similar to estimates by various investigators as compiled by Oort [13].

The horizontal outflow $(1/A) \oint \mathbf{V}_k \cdot \mathbf{n} ds$ shows a significant seasonal variation; its winter value is about three

TABLE 4.—Vertically integrated mean kinetic energy budget from surface to 50 mb. during the 5-yr. period. \bar{k} is in units of 10^5 joules/m². Other quantities are in watts/m².

| Season | Time | \bar{k} | $\frac{\partial \bar{k}}{\partial t}$ | $\frac{1}{A} \oint \mathbf{V}_k \cdot \mathbf{n} ds$ | $\frac{\partial \omega \bar{k}}{\partial p}$ | $-\bar{\mathbf{V}} \cdot \nabla \phi$ | \bar{E} |
|------------------|--------------|-----------|---------------------------------------|--|--|---------------------------------------|-----------|
| Winter* | 00 GMT..... | 21.13 | 0.04 | 4.64 | -0.25 | 10.56 | 6.13 |
| | 12 GMT..... | 21.02 | -0.05 | 5.40 | -0.38 | 8.71 | 3.74 |
| | Average..... | 21.07 | -0.00 | 5.02 | -0.32 | 9.64 | 4.94 |
| Summer** | 00 GMT..... | 12.09 | -0.02 | 1.71 | -0.03 | 7.78 | 6.11 |
| | 12 GMT..... | 12.18 | -0.03 | 1.71 | 0.00 | 2.19 | 2.50 |
| | Average..... | 12.14 | -0.03 | 1.71 | -0.01 | 4.98 | 3.31 |
| Annual Mean..... | 00 GMT..... | 16.61 | .01 | 3.18 | -0.14 | 9.17 | 6.12 |
| | 12 GMT..... | 16.60 | -0.04 | 3.56 | -0.19 | 5.45 | 2.12 |
| | Average..... | 16.60 | -0.01 | 3.37 | -0.17 | 7.31 | 4.12 |

*October, November, December, January, February, and March.

**April, May, June, July, August, and September.

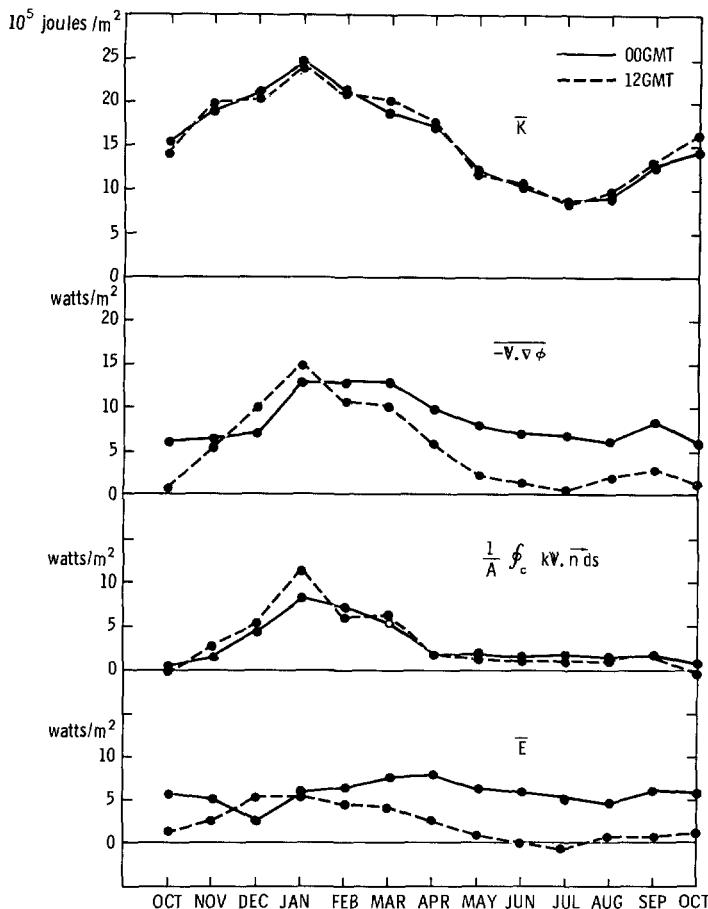


FIGURE 11.—Mean monthly variation of the vertically integrated kinetic energy parameters for the 5-yr. period \bar{k} energy level, $-\bar{V} \cdot \nabla \phi$ generation, $(1/A) \oint_c \mathbf{V}_k \cdot \mathbf{n} ds$ horizontal outflow, and \bar{E} dissipation.

times its summer value. However, the diurnal variation of this term is not significant. During the winter 52 percent of the generated kinetic energy is advected out of North America to the North Atlantic as indicated by the ratio of $(1/A) \oint_c \mathbf{V}_k \cdot \mathbf{n} ds$ to $-\bar{V} \cdot \nabla \phi$; this becomes 34 percent for summer, and 46 percent on an annual basis. Those portions of the advected kinetic energy generated over the continent are assumed to be dissipated beyond the continental boundary.

With the lower and upper boundary condition of $\omega=0$ at the surface and the top of the atmosphere, the vertical transport term $\partial \omega k / \partial p$ should vanish if it is integrated for the entire vertical column of the atmosphere. The integral of the computed $\partial \omega k / \partial p$ from the surface to 50 mb. is negligibly small in the winter and almost vanishes in the summer. The small amount of the vertical transport term which remains in the winter after vertical integration may be explained by the large upward extent of the jet stream level above 50 mb. in winter. During that season some kinetic energy is transported downward from the layer above 50 mb.

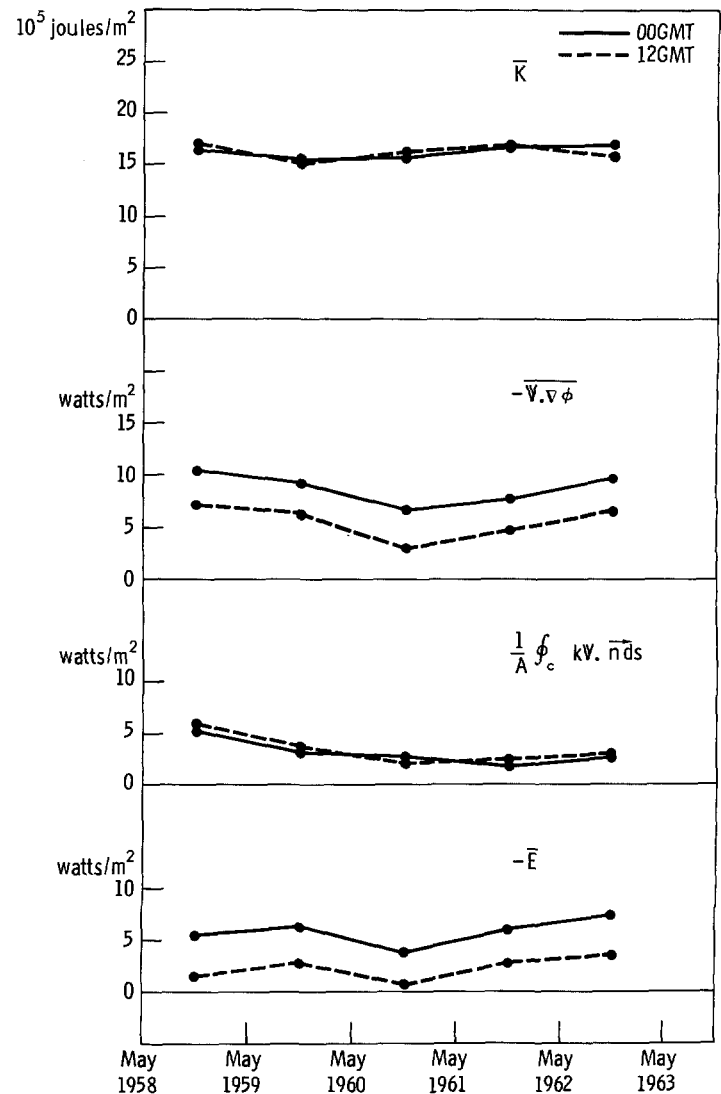


FIGURE 12.—Yearly variation of the annual mean of the vertically integrated kinetic energy parameters for the 5-yr. period \bar{k} energy level, $-\bar{V} \cdot \nabla \phi$ generation, $(1/A) \oint_c \mathbf{V}_k \cdot \mathbf{n} ds$ horizontal outflow, \bar{E} dissipation.

As discussed elsewhere in this paper, there is a significant diurnal variation of the generation $-\bar{V} \cdot \nabla \phi$. The higher generation at 00 GMT than at 12 GMT is especially pronounced during the summer. The ratio of the generation at 00 GMT to that at 12 GMT is 1.00:0.82 for the winter, 1.00:0.28 for the summer, and 1.00:0.59 for the annual mean.

In the previous studies (Kung [10,11]) only the 00 GMT data were employed. As a result, relatively high generation and dissipation values were obtained for the summer months in comparison with the winter months. When the 12 GMT data are used along with 00 GMT data, the average of the 00 and 12 GMT budget shows a more reasonable difference between the winter and summer values of the generation and dissipation. The ratio of the winter and

summer generation is 1.00:0.52, while that between the winter and summer dissipation is 1.00:0.67.

The averages of the 00 and 12 GMT dissipation values, 4.94 watts/m.² for the winter, 3.31 watts/m.² for the summer, and 4.12 watts/m.² for the multi-annual mean, may be tentatively regarded as approximations to the hemispherical values, since to a certain degree the regional effect of the significant diurnal variation averages out. However, those dissipation values may be an underestimate as indicated by some negative dissipation values above the jet core level (see section 3 and tables 1 through 3).

Assuming that the planetary boundary layer is represented by the lowest 100-mb. layer of the atmosphere, the annual mean value of the dissipation in the boundary layer is 2.07 watts/m.² according to the listed values in table 3. This is 50.2 percent of the total annual dissipation 4.12 watts/m.². The boundary layer dissipation 2.07 watts/m.² compares well with the previously estimated 1.87 watts/m.² (Kung [10]) with Lettau's [12] boundary layer model. With this 2.07 watts/m.² boundary layer dissipation, the free atmosphere dissipation will be 2.05 watts/m.², or 49.8 percent of the total dissipation.

Ideally for the long period on the global or hemispherical basis, the atmospheric energy cycle requires the net generation of the available potential energy, the net generation of the kinetic energy, and the dissipation of the kinetic energy to be equal. Oort [13], by compiling various sources of observational studies (also see Krueger, Winston, and Haines [9], Saltzman [15], Saltzman and Fleisher [16, 17], Teweles [19], Wiin-Nielsen [21], and Wiin-Nielsen, Brown, and Drake [22]), gave 2.3 watts/m.² as the currently accepted value for the annual net generation of available potential and kinetic energies and for the kinetic energy dissipation. An annual dissipation of 4.12 watts/m.², which may be an underestimate, is nearly twice the currently accepted value. Although we cannot exclude the possibility of bias produced by confining this study within the North American Continent, an underestimate in the currently accepted value is very probable. The majority of the currently available observational studies of the energy conversions are dependent on vertical motion which is calculated by the adiabatic, quasi-geostrophic models using an operationally modified and smoothed geopotential field. Recently Dutton and Johnson [3] estimated the diabatic generation of the zonal available potential energy as 5.6 watts/m.² with their exact theory. With the dissipation 4.12 watts/m.² in this study to be taken as the net generation of available potential energy, their estimation implies the destruction of the eddy available potential energy at the rate of 1.48 watts/m.²

6. CONCLUDING REMARKS

By using the wind and geopotential data observed twice a day at 00 and 12 GMT over North America during

a 5-yr. period, a significant and consistent diurnal variation in the computed generation and dissipation of the kinetic energy is observed. The larger generation and dissipation in the lower troposphere and at the jet stream level at 00 GMT than at 12 GMT is especially pronounced during the summer.

With the use of the twice-a-day observations for an extended period, the regional values of the large-scale energetics may be an approximation to the hemispheric values. However, uncertainty remains because of the possible effects of semidiurnal variations and the unconfirmed radiation errors in the radiosonde observations. The previously reported (Kung [11]) characteristics of the vertical profile of the kinetic energy balance with the 00 GMT data for the 11 months are essentially verified in this study; namely, there are maxima in the generation $-\mathbf{V} \cdot \nabla \phi$ and dissipation \bar{E} in the planetary boundary layer and at the jet stream level. However, the actual shape of the profiles was modified by adding the 12 GMT observations, and became closer to that predicted in the numerical experiment by Smagorinsky, Manabe, and Holloway [18].

The kinetic energy level \bar{k} , generation $-\mathbf{V} \cdot \nabla \phi$, horizontal transport $(1/A) \oint_c \mathbf{V} k \cdot \mathbf{n} ds$, and dissipation \bar{E} all show the clear march of the seasons in the annual cycle. The year-to-year variation of the energy parameters is significant, although the diurnal variation (difference of 00 and 12 GMT values) is nearly constant from year to year.

We cannot exclude the possibility of bias caused by confining this study within a continent, even after combining 00 and 12 GMT values. The significance of undetected eddies with the current density of the observational network is an open question. However, the computation in this study, which uses actual wind data along with the geopotential gradient, is not restricted by the operationally obtained vertical velocity. With some possibility of underestimation, the multi-annual mean of the energy dissipation is 4.12 watts/m.², which balances the local change -0.01 watts/m.², horizontal outflow 3.37 watts/m.², the vertical transport -0.17 watts/m.², and the generation 7.31 watts/m.² in the kinetic energy equation. The dissipation 4.12 watts/m.², which ideally should be equal to the long-term average of the net generations of the available potential energy and kinetic energy, is significantly higher than the currently accepted values.

ACKNOWLEDGMENTS

The author is greatly indebted to Professor V. P. Starr of the Massachusetts Institute of Technology for his suggestion to make an extensive use of 12 GMT data along with 00 GMT data, and also for his valuable comments in revising the manuscript. The kind arrangement of Mr. H. M. Frazier of The Travelers Research Center, Inc., for our use of the data tapes is sincerely acknowledged.

The author is very grateful to Dr. E. M. Rasmusson, Dr. K. Bryan, and Mr. S. Hellerman for their discussions and for reviewing the original manuscript.

Continuous encouraging interest and comments of Dr. J. Smagorinsky, and Dr. S. Manabe, and also of Professor J. A. Dutton of the Pennsylvania State University are greatly appreciated.

Thanks are due to Mr. W. H. Moore for his technical help, and to Mrs. C. Bunce and Mrs. M. Fox for their preparation of the manuscript.

REFERENCES

1. W. Bleeker and M. J. Andre, "On the Diurnal Variation of Precipitation, Particularly over the Central U.S.A., and Its Relation to Large-Scale Orographic Circulation Systems," *Quarterly Journal of the Royal Meteorological Society*, vol. 77, No. 332, Apr. 1951, pp. 260-271.
2. R. C. Curtis and H. A. Panofsky, "The Relation Between Large-Scale Vertical Motion and Weather in Summer," *Bulletin of the American Meteorological Society*, vol. 39, No. 10, Oct. 1958, pp. 521-531.
3. J. A. Dutton and D. R. Johnson, "The Theory of Available Potential Energy and a Variation Approach to Atmospheric Energetics," *Advances in Geophysics*, vol. 12, 1967, pp. 333-436.
4. F. G. Finger, M. F. Harris, and S. Teweles, "Diurnal Variation of Wind, Pressure, and Temperature in the Stratosphere," *Journal of Applied Meteorology*, vol. 4, No. 5, Oct. 1965, pp. 632-635.
5. M. F. Harris, F. G. Finger, and S. Teweles, "Frictional and Thermal Influence in the Solar Semidiurnal Tide," *Monthly Weather Review*, vol. 94, No. 7, July 1966, pp. 427-447.
6. W. S. Hering and T. R. Borden, Jr., "Diurnal Variations in the Summer Wind Field over the Central United States," *Journal of the Atmospheric Sciences*, vol. 19, No. 1, Jan. 1962, pp. 81-86.
7. E. O. Holopainen, "Investigation of Friction and Diabatic Processes in the Atmosphere," *Paper No. 101*, Institute of Meteorology, University of Helsinki, 1964, 47 pp.
8. C. E. Jensen, "Energy Transformation and Vertical Flux Processes over the Northern Hemisphere," *Journal of Geophysical Research*, vol. 66, No. 4, Apr. 1961, pp. 1145-1156.
9. A. F. Krueger, J. S. Winston, and D. A. Haines, "Computation of Atmospheric energy and its transformation for the Northern Hemisphere for a Recent Five-Year Period," *Monthly Weather Review*, vol. 93, No. 4, Apr. 1965, pp. 227-238.
10. E. C. Kung, "Kinetic Energy Generation and Dissipation in the Large-Scale Atmospheric Circulation," *Monthly Weather Review*, vol. 93, No. 2, Feb. 1966, pp. 67-82.
11. E. C. Kung, "Large-Scale Balance of Kinetic Energy in the Atmosphere," *Monthly Weather Review*, vol. 94, No. 11, Nov. 1966, pp. 627-640.
12. H. H. Lettau, "Theoretical Wind Spirals in the Boundary Layer of a Barotropic Atmosphere," *Beiträge zur Physik der Atmosphäre*, vol. 35, No. 3/4, 1962, pp. 195-212.
13. A. H. Oort, "On Estimates of the Atmospheric Energy Cycle," *Monthly Weather Review*, vol. 92, No. 11, Nov. 1964, pp. 483-493.
14. E. M. Rasmusson, "Atmospheric Water Vapor Transport and the Water Balance of North America: Part 1. Characteristics of the Water Vapor Flux Field," *Monthly Weather Review*, vol. 95, No. 7, July 1967, pp. 403-426.
15. B. Saltzman, "The Zonal Harmonic Representation of the Atmospheric Energy Cycle—A Review of Measurements," *Report TRC-9*, The Travelers Research Center, Sept. 1961, 19 pp.
16. B. Saltzman and A. Fleisher, "Spectrum of Kinetic Energy Transfer due to Large-Scale Horizontal Reynolds Stress," *Tellus*, vol. 12, No. 1, Feb. 1960, pp. 110-111.
17. B. Saltzman and A. Fleisher, "Further Statistics of the Modes of Release of Available Potential Energy," *Journal of Geophysical Research*, vol. 66, No. 7, July 1961, pp. 2271-2273.
18. J. Smagorinsky, S. Manabe, and J. L. Holloway, Jr., "Numerical Results From a Nine-Level General Circulation Model of the Atmosphere," *Monthly Weather Review*, vol. 93, No. 12, Dec. 1965, pp. 727-768.
19. S. Teweles, "Spectral Aspects of the Stratospheric Circulation During the IGY," *Report No. 8*, Dept. of Meteorology, Massachusetts Institute of Technology, Jan. 1963, 191 pp.
20. The Travelers Research Center, Inc., "Northern Hemisphere Station Aerological Data Tables of Monthly Reporting Frequencies by Parameter/Level (Including 60-Month Sums) for the Period May 1958-April 1963," *Report 7453-165*, Apr. 1965, 61 tables.
21. A. Wiin-Nielsen, "A Study of Energy Conversion and Meridional Circulation for the Large-Scale Motion in the Atmosphere," *Monthly Weather Review*, vol. 90, No. 8, Aug. 1962, pp. 311-323.
22. A. Wiin-Nielsen, J. A. Brown, and M. Drake, "On Atmospheric Energy Conversion Between the Zonal Flow and the Eddies," *Tellus*, vol. 15, No. 3, Aug. 1963, pp. 261-279.

[Received April 28, 1967; revised June 26, 1967]